Supplementary Information

Revealing the stoichiometric tolerance of lead tri-halide perovskite thin-films

Alexandra J. Ramadan, Maryline Ralaiarisoa, Fengshuo Zu, Luke A. Rochford, Bernard Wenger, Norbert Koch, Henry J. Snaith

Contents

	Cs	Pb	Br	Br expected in the final sample
$PbBr_2$	0	1	1.78	2
0.01	0.09	1	1.86	2.01
0.1	0.14	1	1.92	2.1
0.25	0.32	1	2.29	2.25
0.5	0.51	1	2.50	2.5
0.75	0.7	1	2.94	2.75
1	1.09	1	2.84	3
1.25	1.62	1	2.77	3.25
1.5	1.99	1	3.18	3.5
CsBr	1	0	0.5	1

Table S1 – Chemical stoichiometry of $CsPbBr_3$ thin films as determined by fitting of high resolution x-ray photoemission spectroscopy measurements.

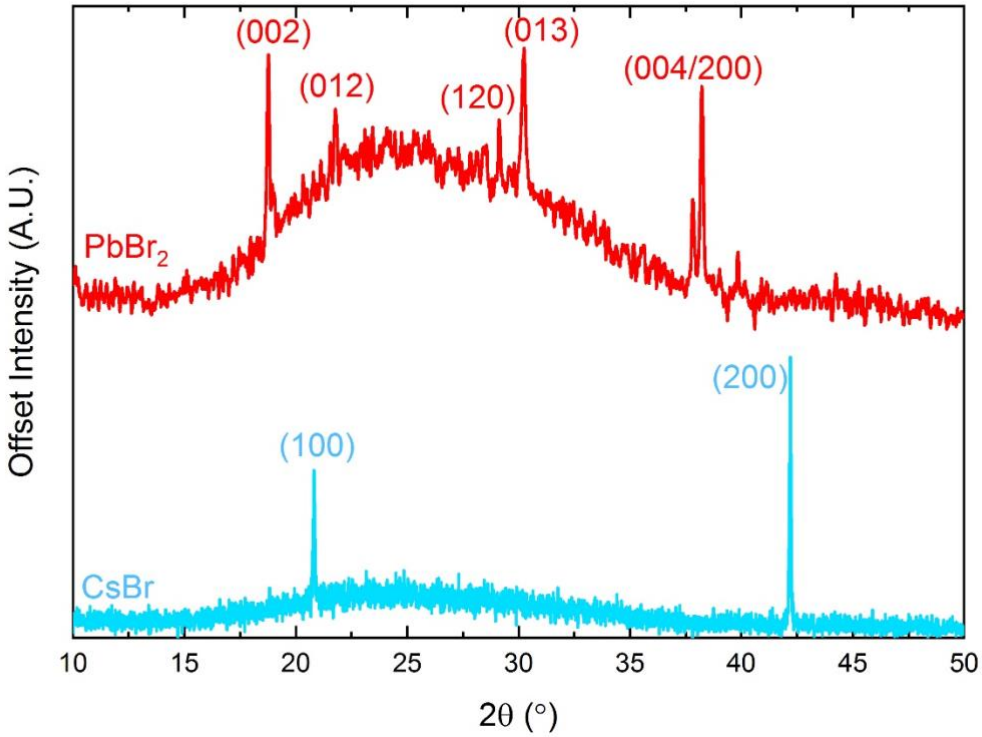

Figure S1 – X-ray diffraction patterns of CsBr and $PbBr_2$ thin films on pedot:PSS/ITO glass.

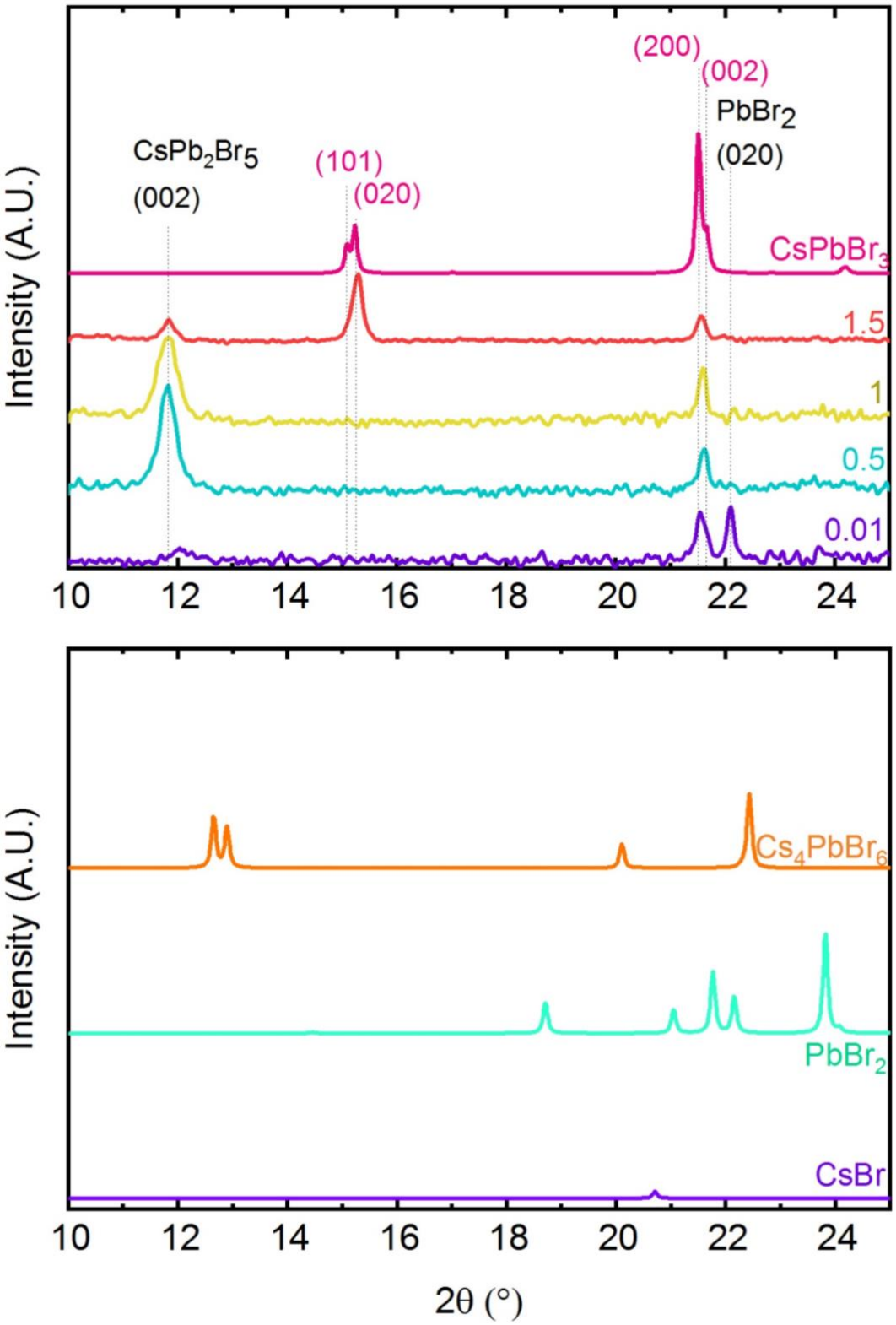

Figure S2 – X-ray diffraction patterns (between 2θ = 10 - 25°) of specific $CsPbBr_3$ compositions with comparison to published crystal structures of $CsPbBr_3$, Cs_4PbBr_6, CsBr and $PbBr_2$. The peak positions correlating to $CsPb_2Br_5$ are marked on the diffraction patterns (reference [1])as a crystal structure for this material is not yet available.

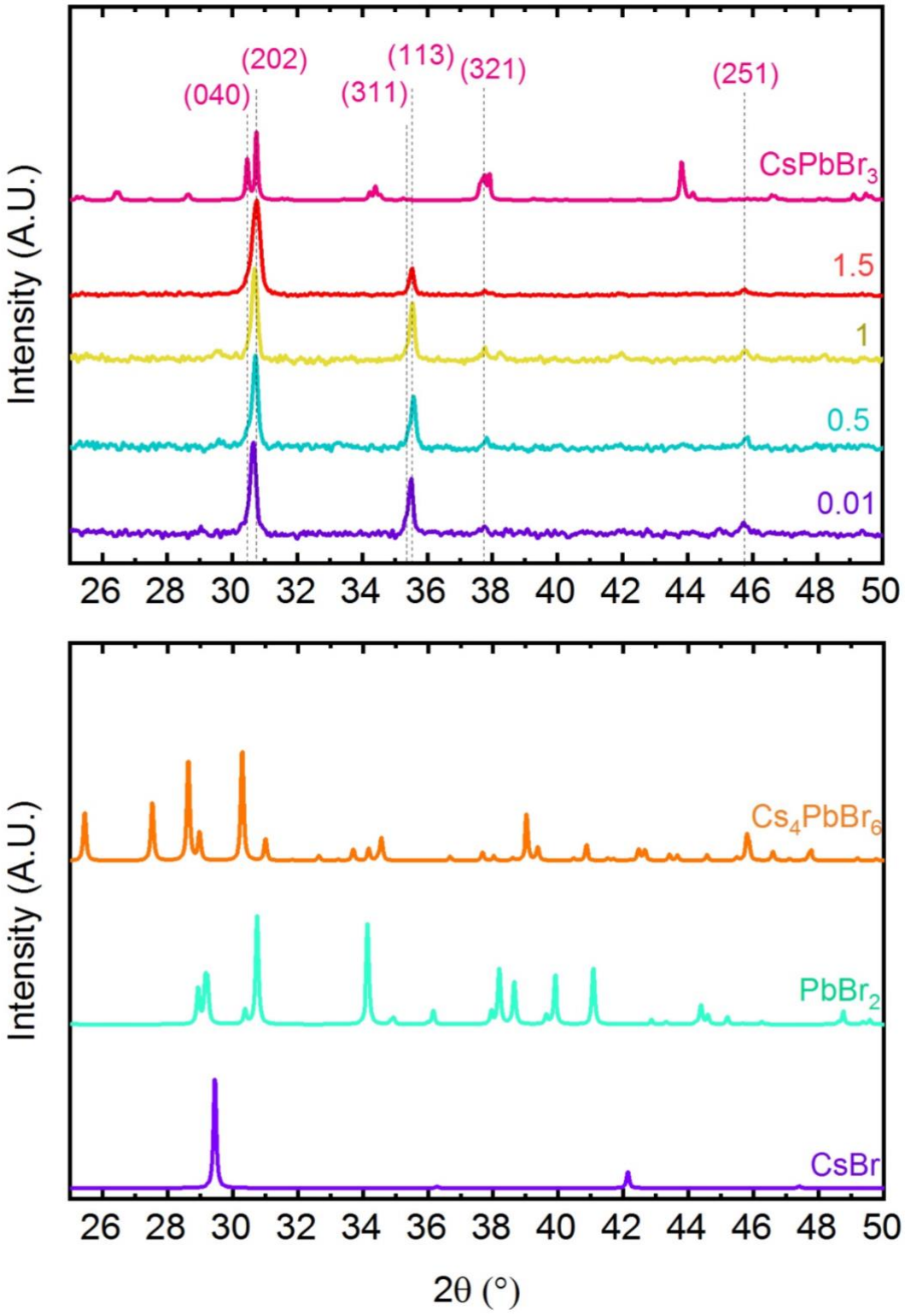

Figure S3 – X-ray diffraction patterns (between 2θ = 25 - 50°) of specific $CsPbBr_3$ compositions with comparison to published crystal structures of $CsPbBr_3$, Cs_4PbBr_6, CsBr and $PbBr_2$.

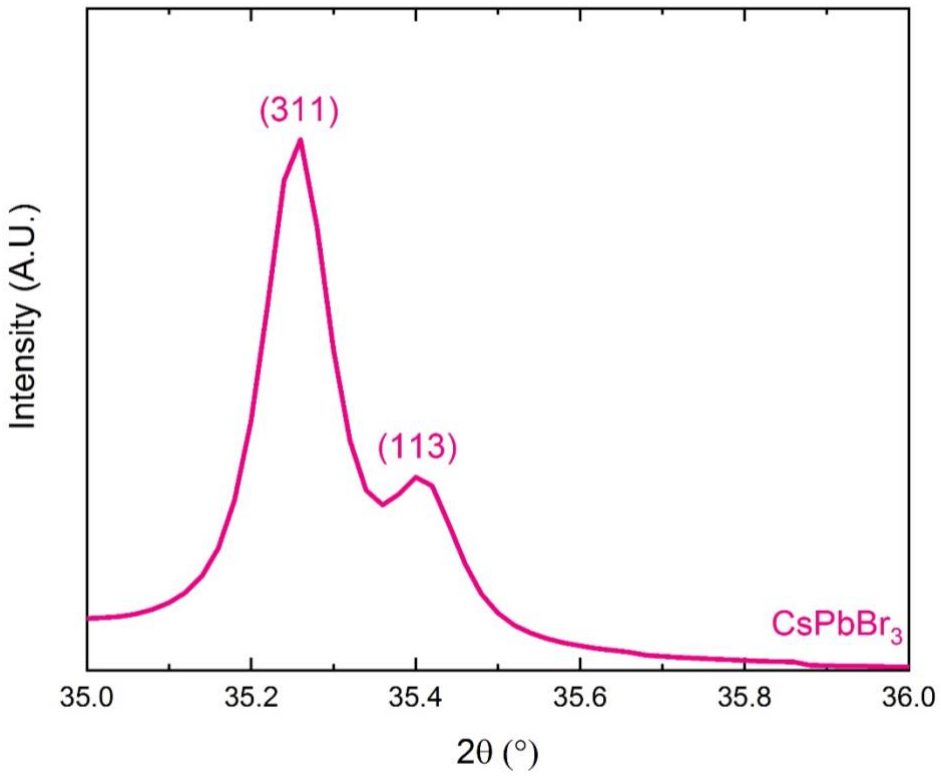

Figure S4 – Enlarged image of simulated powder pattern (2θ = 35 - 36°) of $CsPbBr_3$ orthorhombic crystal structure.[2]

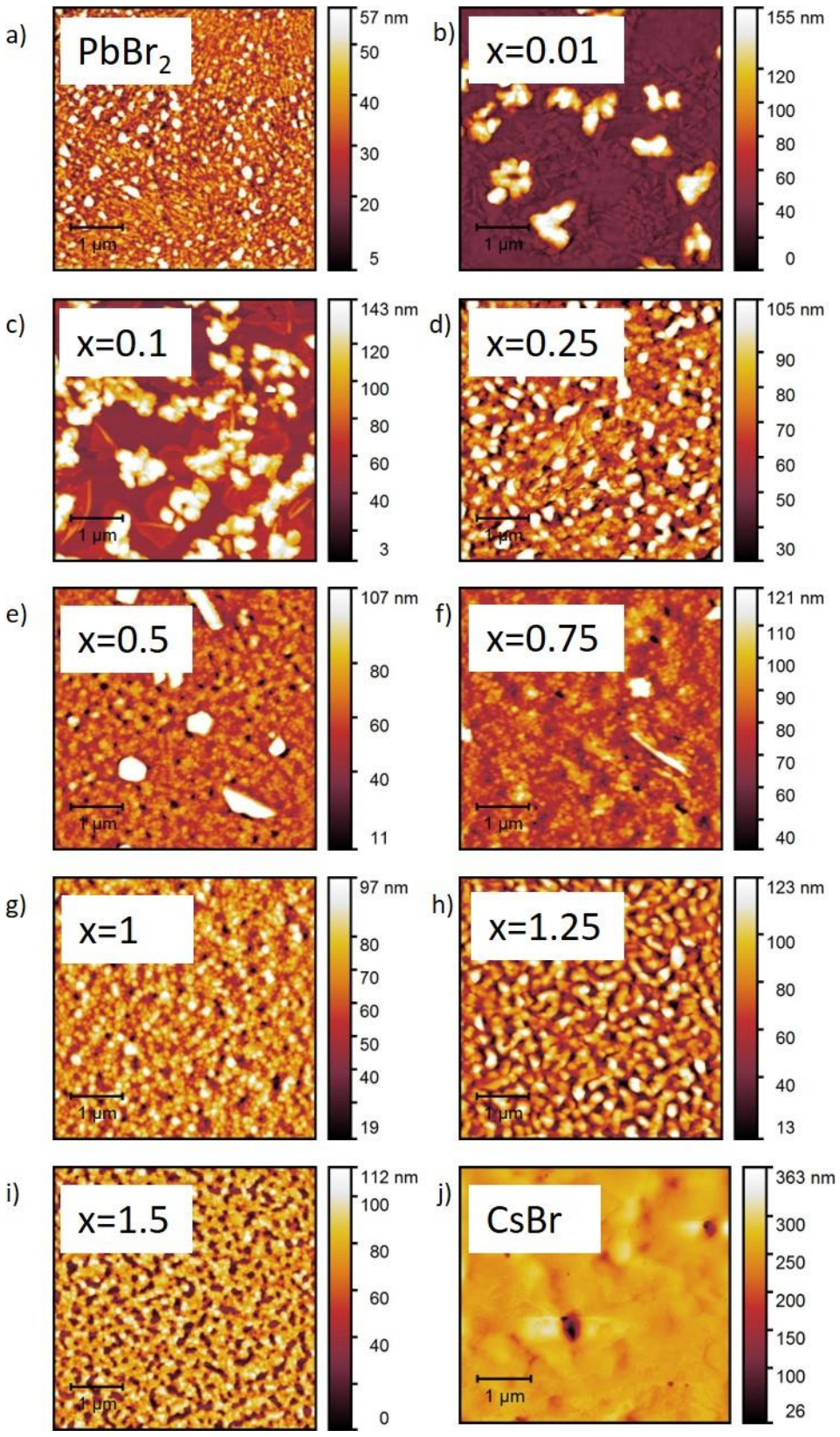

Figure S5 – Atomic force microscopy images showing the topography of $CsPbBr_3$ films with increasing CsBr content.

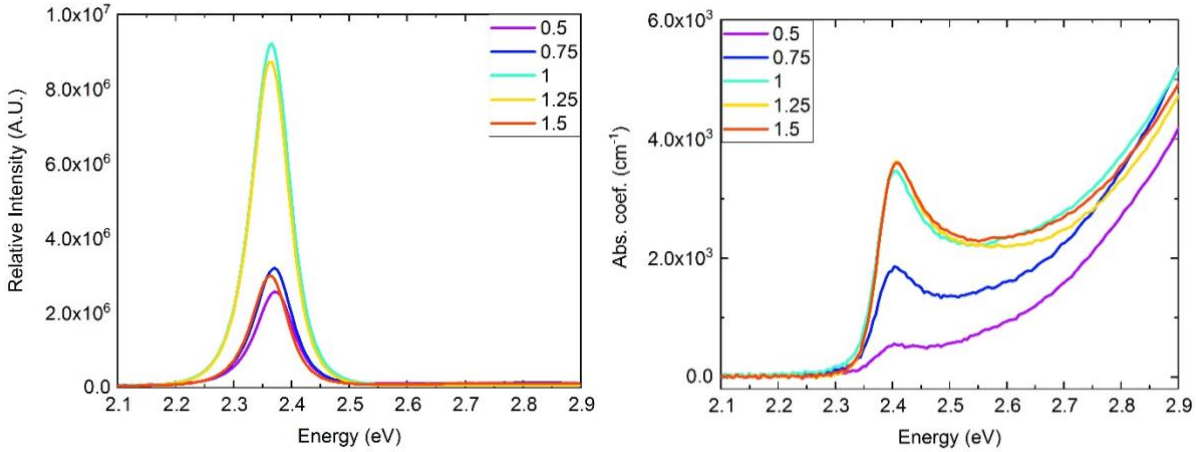

Figure S6 – Steady state photoluminescence spectra (left) and UV-Vis spectra (right) and of $CsPbBr_3$ films with different CsBr content deposited on PEDOT:PSS/ITO glass.

x=	Absorption Maximum (nm)	Emission Maximum (nm)	Optical Band Gap (eV)
0.5	516	523	2.48
0.75	516	523	2.49
1	516	525	2.49
1.25	516	525	2.5
1.5	516	525	2.5

Table S2 – Summary of absorption and emission maxima for all $CsPbBr_3$ films with different CsBr content deposited on PEDOT:PSS/ITO glass.

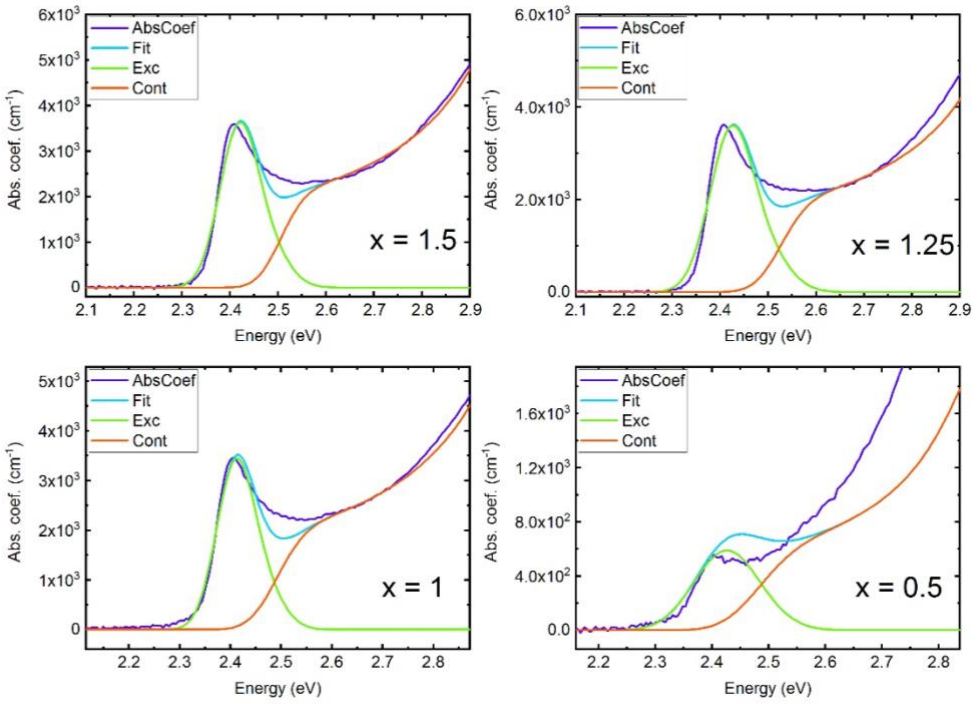

Figure S7 – Elliott model fitting of UV-vis spectra of $CsPbBr_3$ films deposited on Pedot:PSS/ITO glass.

Supplementary note 1 - Estimation of the continuum band gap from optical absorption spectra.

As discussed in the manuscript, the CBM and VBM, evaluated from IPES and UPS respectively, are characteristic of the continuum of states in the conduction and valence bands. The conventional method to estimate the bandgap of a direct gap semiconductor is to perform a Tauc plot. However, in the presence of a large excitonic peak, as for the $CsPbBr_3$ films investigated here, this method will give a value that is substantially lower than the absorption edge due to the continuum states. Therefore, we use Elliott's model'sto separate the contribution from the excitonic peak and the continuum.[3] To fit the data we follow the formulation of Davies *et al.* and add a anharmonicity parameter to account for the fast rise in absorption above band gap.[4,5] The excitonic lines and continuum step are broadened by convolution with gaussian functions.

The experimental spectra of the films were measured in an integration sphere (see experimental section). In order to maintain the same crystallisation conditions than for the samples prepared for the other characterisation methods (XRD, XPS, UPS, IPES), the perovskite films were coated on a thin PEDOT:PSS layer. In Figure S2, we show the absorption spectra obtained by combining the experimental total transmittance (T_t) and total reflectance (R_t), $\alpha = -\frac{1}{d}\ln\left(\frac{T_t}{1-R_t}\right)$, where α is the

absorption coefficient and *d* the thickness of the film. Due to the presence of the PEDOT:PSS film, the spectra show a relatively large absorption above 500 nm, which needs to be corrected in order to improve the quality of the data for fitting with Elliott's model. To fully account for the reflections at all interfaces, an optical model taking into account the optical constants of each material and their exact thicknesses should be used (*e.g* transfer matrix method). Here, we use a simplified approach which consists in the subtraction of the contribution of PEDOT:PSS estimated from its absorption coefficient and scaled for a given thickness which is optimised for each sample. The optimal thickness for the polymer is found to be much lower (8-14 nm) than measured with a profilometer (30 nm), which suggests that some PEDOT:PSS is dissolved when the perovskite is spin-coated. We note also that we neglect changes in reflection due to the refractive index contrast (polymer/air vs polymer/perovskite). The absorption coefficient is calculated as:

$$\alpha = -\frac{1}{d}\ln\left(\frac{T_c}{1-R_t}\right)$$

$$T_c = T_t - \left(1 - exp\left(A_p d_p\right)\right)$$

Where T_c is the corrected transmittance, A_p is the absorption coefficient of the polymer (measured from a PEDOT:PSS film deposited on glass) and d_p is the thickness of the polymer film which here is an adjustable parameter.

x=	Cs $3d_{5/2}$	Pb $4f_{7/2}$	Br $3d_{5/2}$
$PbBr_2$		138.8 139.8	68.4
0.01	723.4	138.0	67.8
0.1	723.7	138.1	67.8
0.25	723.9	138.0	67.8
0.5	723.9	138.0	67.8
0.75	723.9	137.8	67.7
1	723.8	137.7	67.6
1.25	723.8	137.7	67.7
1.5	723.8	137.7	67.6
CsBr	724.4 725.3		68.5

Table S3 – Peak positions and full assignments for high resolution XPS scans for all $CsPbBr_3$ thin films.

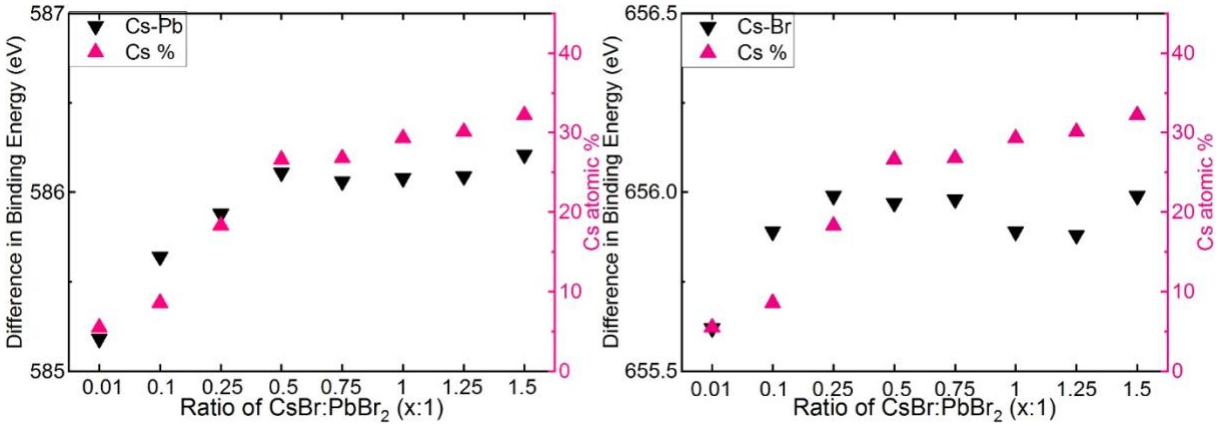

Figure S8 – Plots of the difference in binding energy between two core levels (e.g. Cs – Pb) plotted with respect to the ratio of alkali metal content to $PbBr_2$. This is then plotted alongside the experimentally determined atomic percentage (as determined from fitting of the XPS data).

x=	VBM linear (eV)	VBM log (eV)	IE linear (eV)	IE log (eV)	Work Function (eV)
$PbBr_2$	1.83	1.6	6.61	6.38	4.78
0.01	1.95	1.72	6.62	6.39	4.67
0.1	1.54	1.36	6.51	6.33	4.97
0.25	1.43	1.19	6.38	6.14	4.95
0.5	1.23	0.9	6.4	6.07	5.17
0.75	1.12	0.95	6.68	6.51	4.97
1	1.08	0.8	6.28	6	5.2
1.25	0.95	0.73	6.27	6.05	5.32
1.5	0.9	0.83	6.05	5.98	5.15
CsBr	2.1	2	7.22	7.12	5.12

Table S4 – Valence band maximum (VBM), ionisation energies (IE) and work function values for all samples determined from UPS measurements.

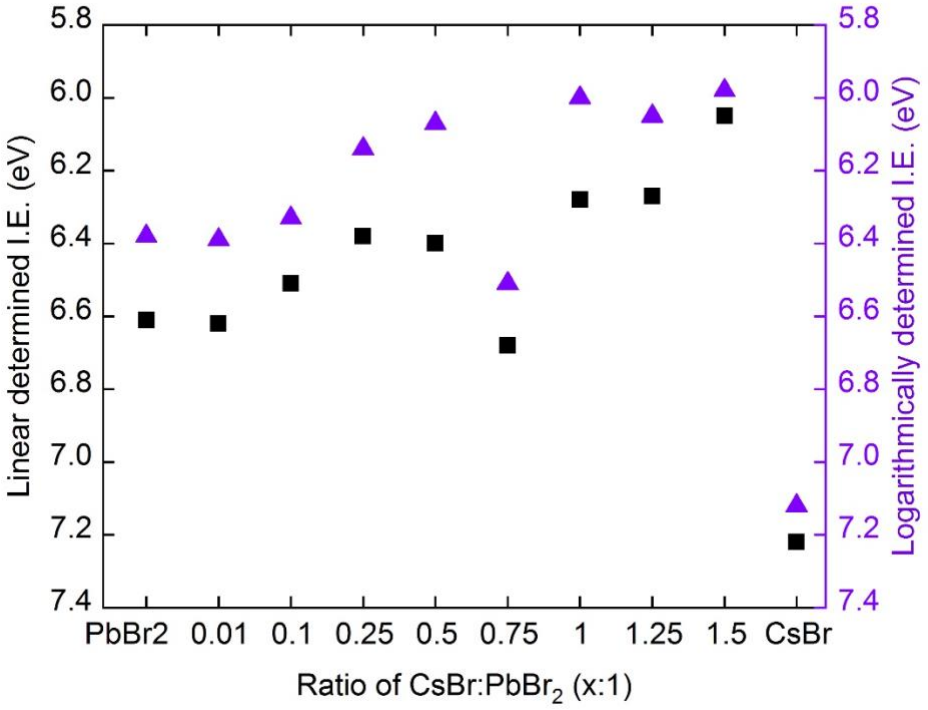

Figure S9 - Plot of ionisation energies for each composition as determined using both a linear and logarithmic plot of UPS spectra.

x=	EAs linear (eV)	Elec. band gap linear (eV)	Elec. band gap log (eV)	Optical band gap (eV)
$PbBr_2$	3.81	2.8	2.57	3.4
0.5	3.59	2.81	2.48	2.48
1	3.79	2.49	2.21	2.49
1.25	3.85	2.42	2.2	2.5
1.5	3.7	2.35	2.28	2.5
CsBr	3.51	3.71	3.61	3.02

Table S5 – The summarized electron affinities (EAs) determined from the UPS and IPES measurements and resulting electronic band gaps.

Fitting of X-ray photoemission spectroscopy data:

X-ray photoemission spectra were fit using the Casa XPS software, peaks were fit using a mixture of Gaussian/Lorentzian (Lorentzian = 30%) line shapes using a Shirley background.

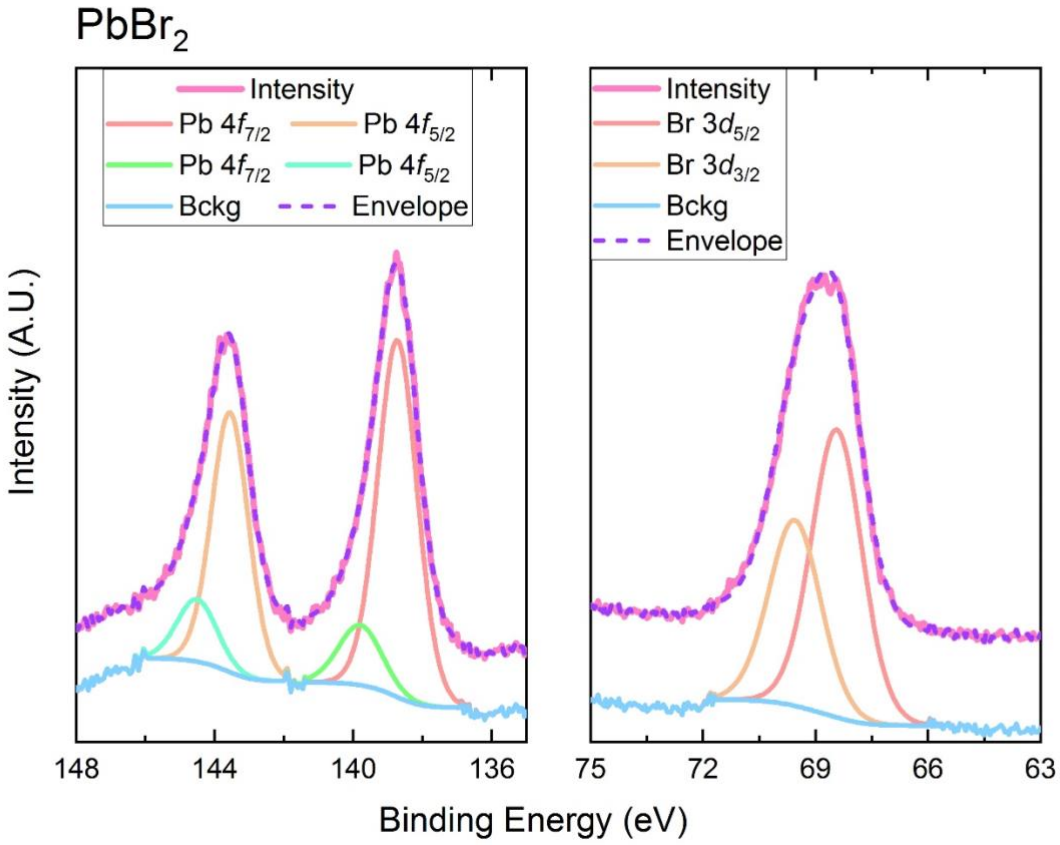

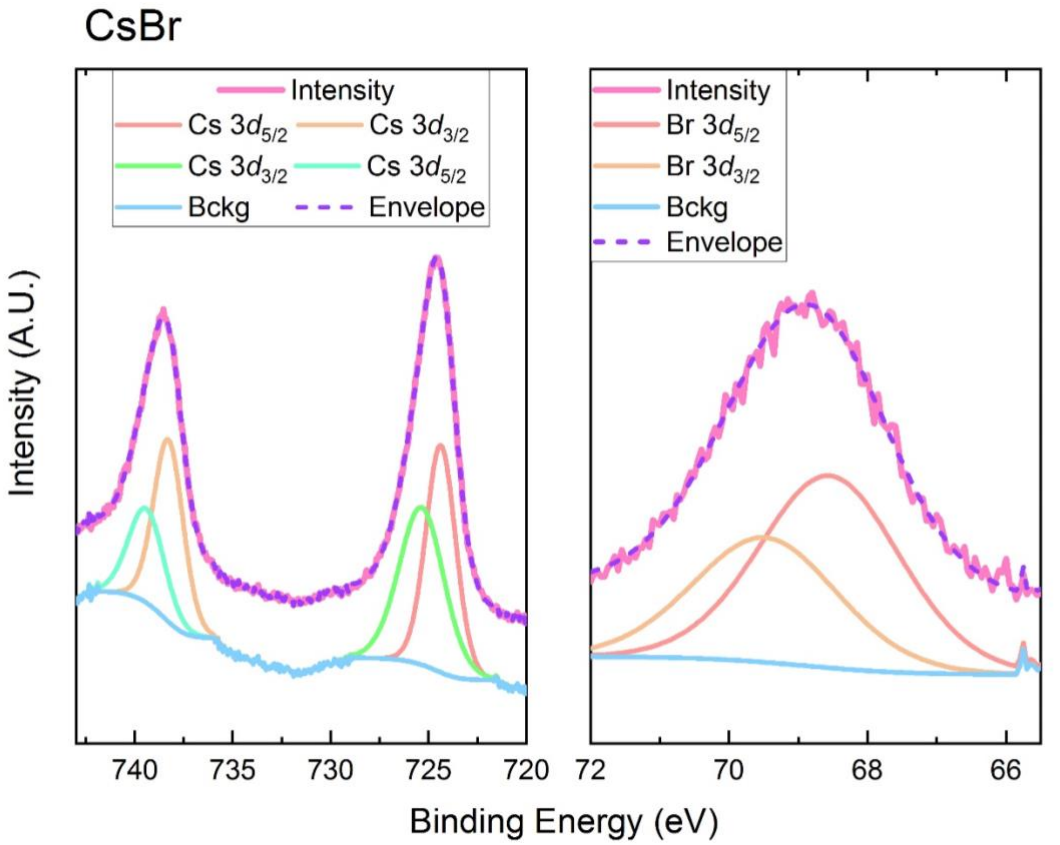

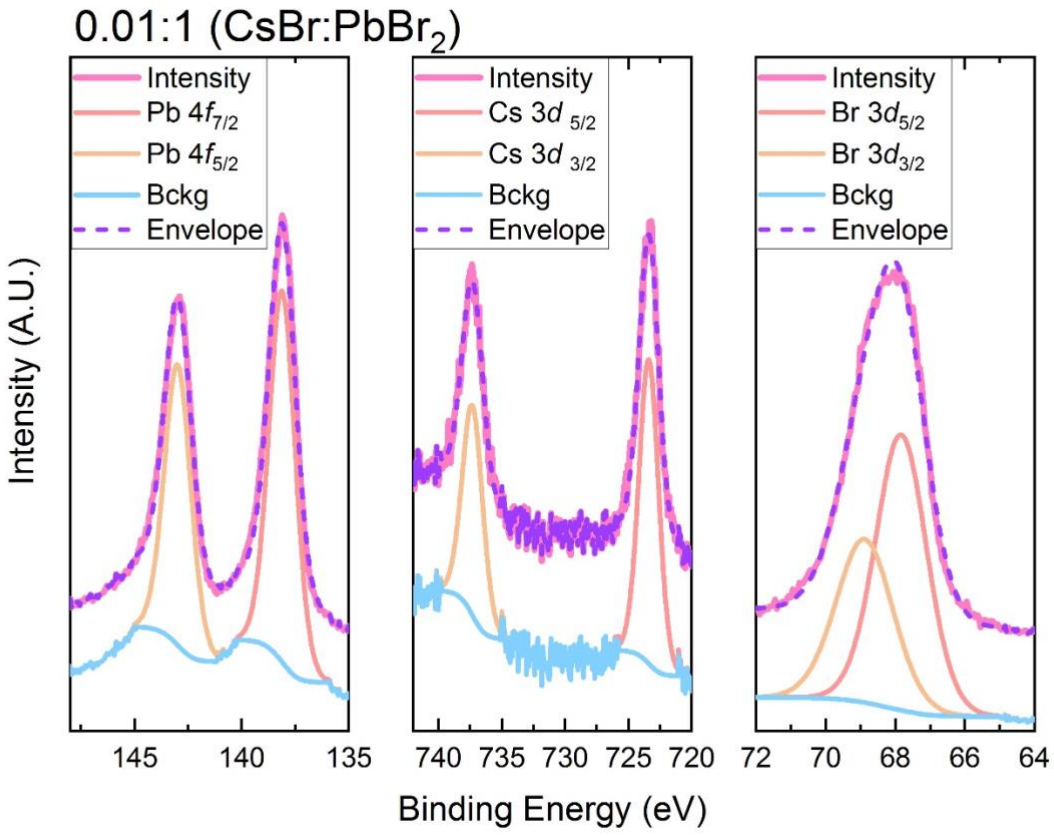
0.01:1 (CsBr:PbBr2)
Intensity
Pb 4f7/2
Pb 4f5/2
Bckg
Envelope
Cs 3d 5/2
Cs 3d 3/2
Br 3d5/2
Br 3d3/2
Intensity (A.U.)
145 140 135
740 735 730 725 720
72 70 68 66 64
Binding Energy (eV)

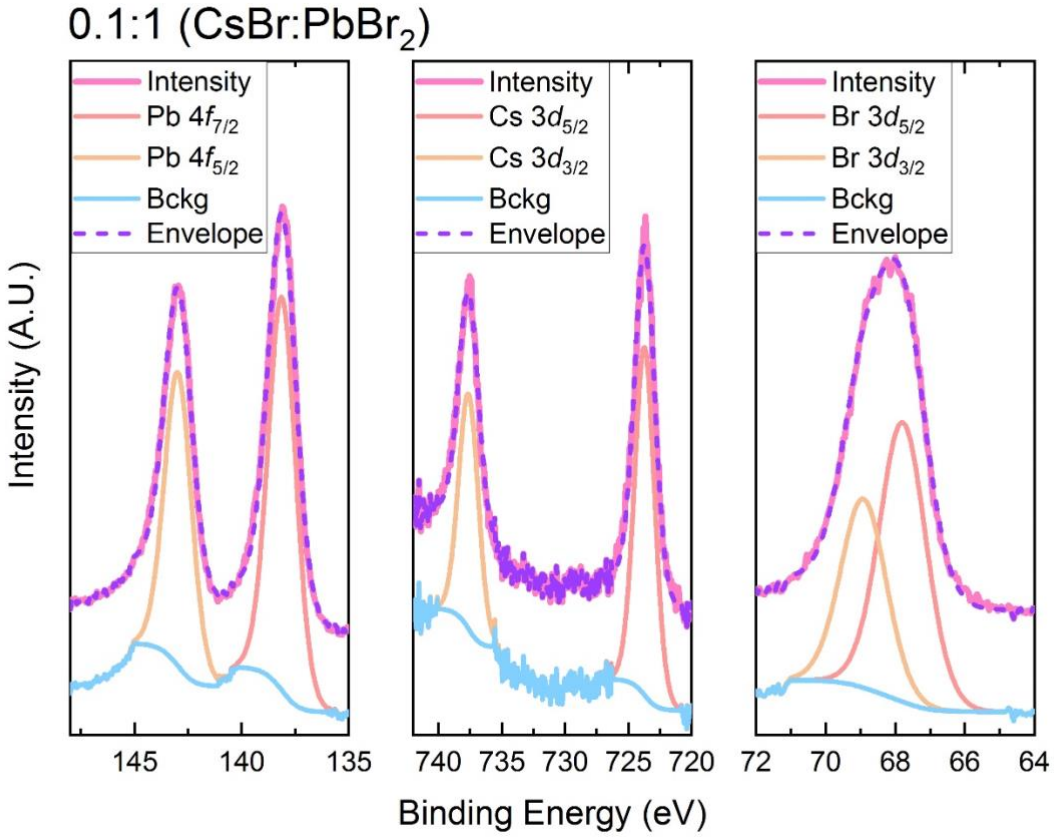
0.1:1 (CsBr:PbBr2)
Intensity
Pb 4f7/2
Pb 4f5/2
Bckg
Envelope
Cs 3d5/2
Cs 3d3/2
Br 3d5/2
Br 3d3/2
Intensity (A.U.)
145 140 135
740 735 730 725 720
72 70 68 66 64
Binding Energy (eV)

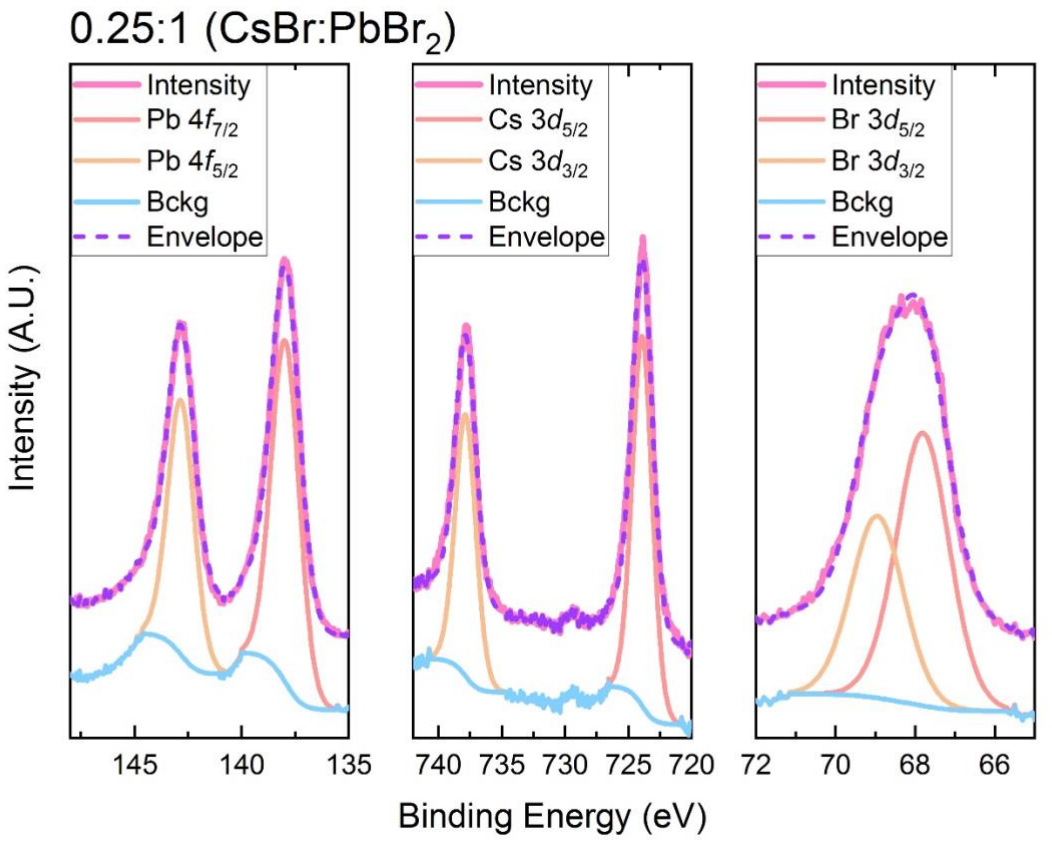
0.25:1 (CsBr:PbBr2)
Intensity
Pb 4f7/2
Pb 4f5/2
Bckg
Envelope
Intensity
Cs 3d5/2
Cs 3d3/2
Bckg
Envelope
Intensity
Br 3d5/2
Br 3d3/2
Bckg
Envelope
Intensity (A.U.)
145
140
135
740
735
730
725
720
72
70
68
66
Binding Energy (eV)

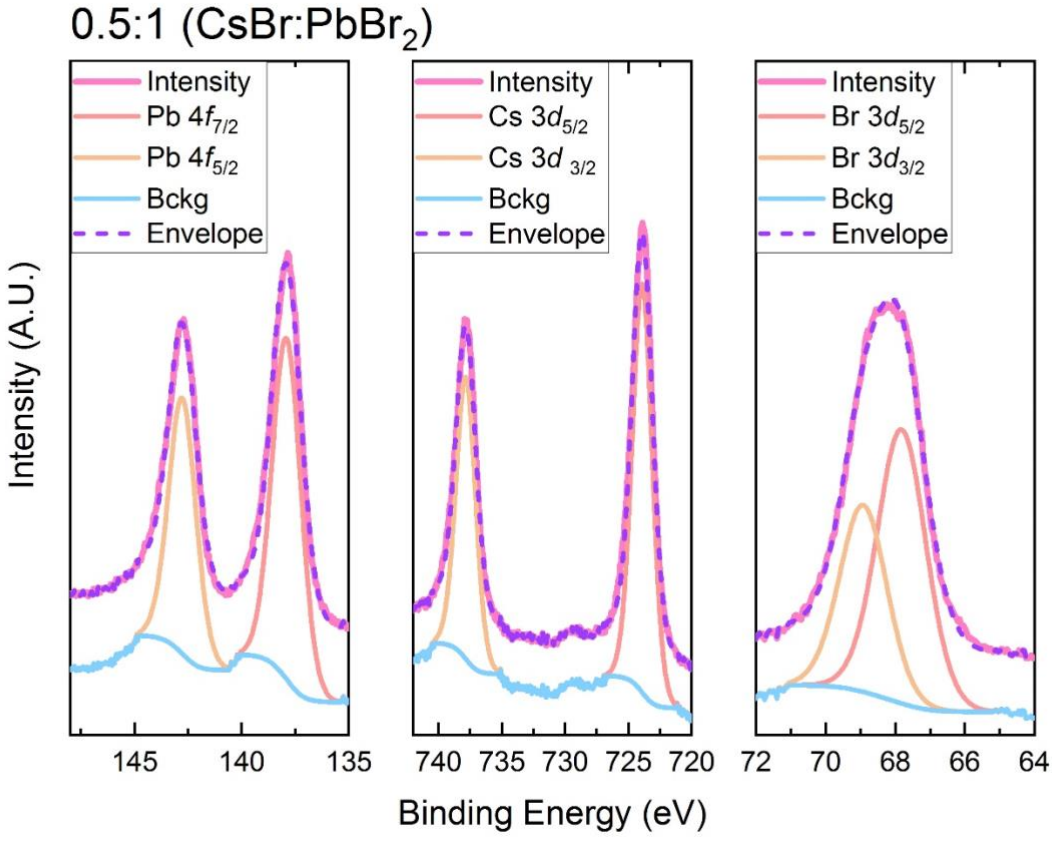
0.5:1 (CsBr:PbBr2)
Intensity
Pb 4f7/2
Pb 4f5/2
Bckg
Envelope
Intensity
Cs 3d5/2
Cs 3d 3/2
Bckg
Envelope
Intensity
Br 3d5/2
Br 3d3/2
Bckg
Envelope
Intensity (A.U.)
145
140
135
740
735
730
725
720
72
70
68
66
64
Binding Energy (eV)

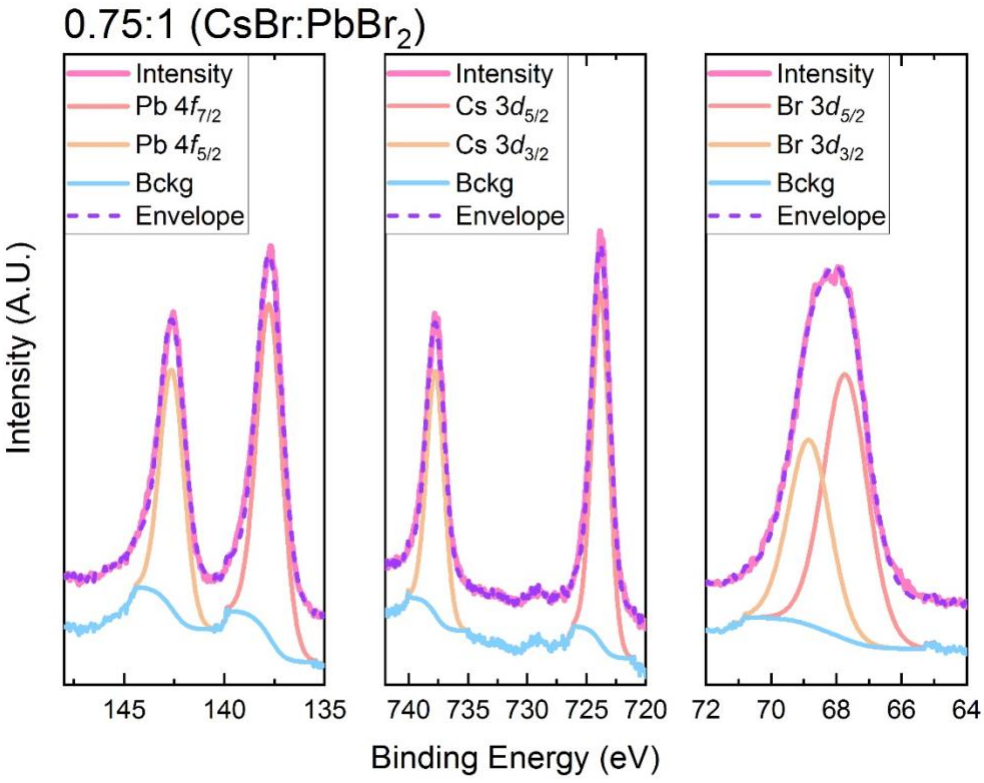
0.75:1 (CsBr:PbBr2)
Intensity
Pb 4f7/2
Pb 4f5/2
Bckg
Envelope
Cs 3d5/2
Cs 3d3/2
Br 3d5/2
Br 3d3/2
Intensity (A.U.)
145
140
135
740
735
730
725
720
72
70
68
66
64
Binding Energy (eV)

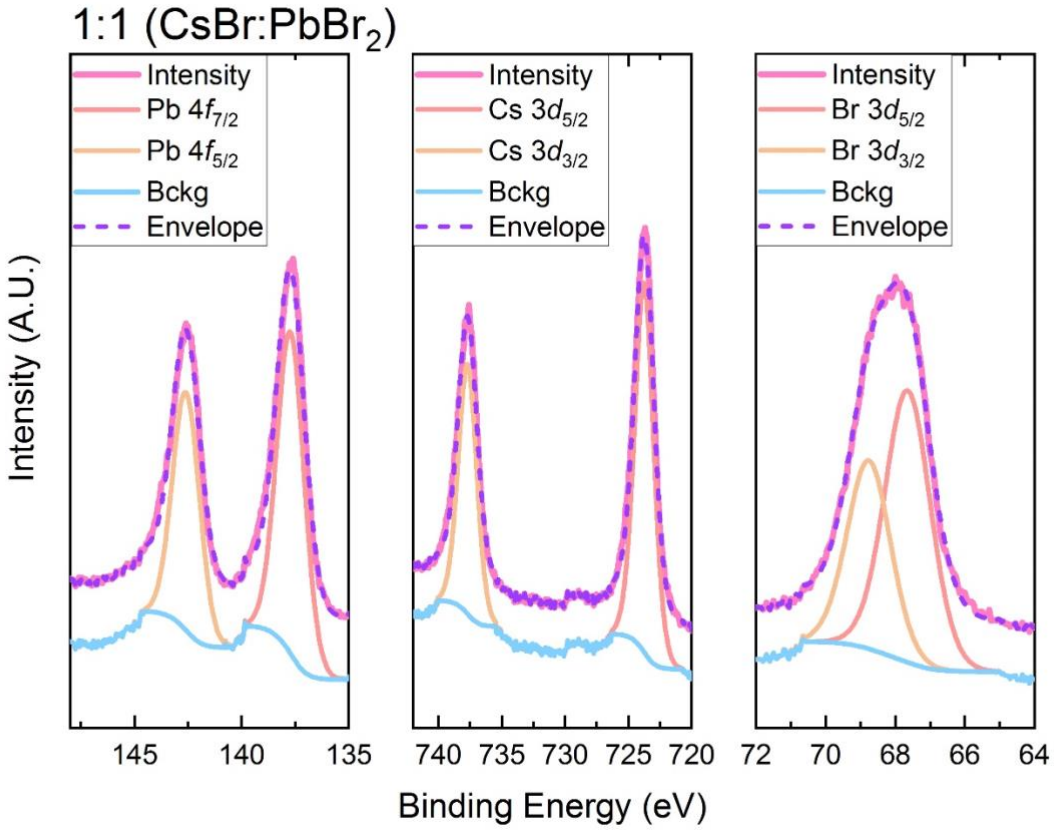
1:1 (CsBr:PbBr2)
Intensity
Pb 4f7/2
Pb 4f5/2
Bckg
Envelope
Cs 3d5/2
Cs 3d3/2
Br 3d5/2
Br 3d3/2
Intensity (A.U.)
145
140
135
740
735
730
725
720
72
70
68
66
64
Binding Energy (eV)

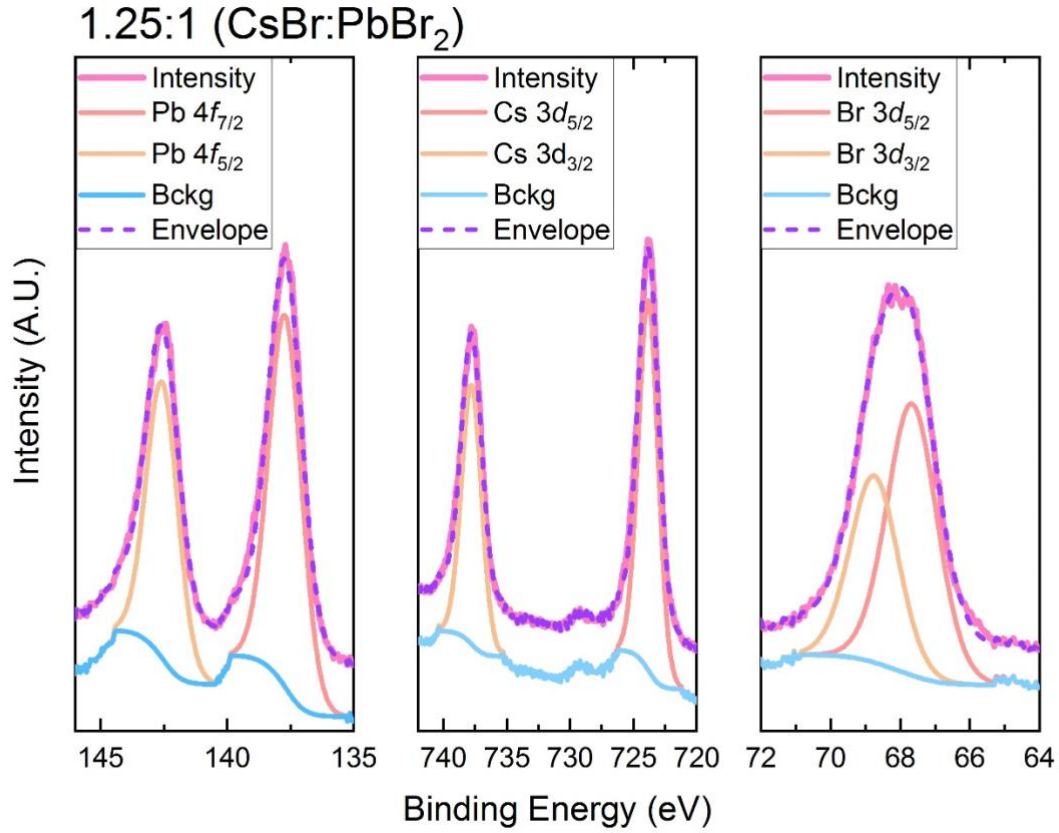
1.25:1 (CsBr:PbBr2)
Intensity
Pb 4f7/2
Pb 4f5/2
Bckg
Envelope
Intensity
Cs 3d5/2
Cs 3d3/2
Bckg
Envelope
Intensity
Br 3d5/2
Br 3d3/2
Bckg
Envelope
Intensity (A.U.)
145
140
135
740
735
730
725
720
72
70
68
66
64
Binding Energy (eV)

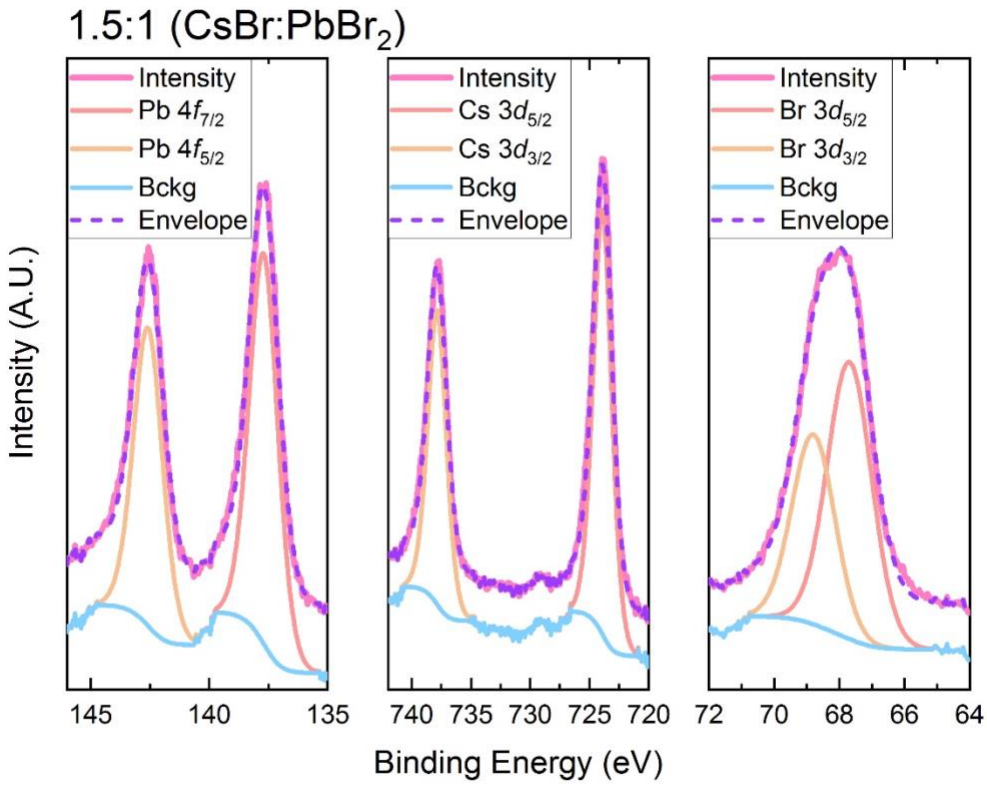
1.5:1 (CsBr:PbBr2)
Intensity
Pb 4f7/2
Pb 4f5/2
Bckg
Envelope
Intensity
Cs 3d5/2
Cs 3d3/2
Bckg
Envelope
Intensity
Br 3d5/2
Br 3d3/2
Bckg
Envelope
Intensity (A.U.)
145
140
135
740
735
730
725
720
72
70
68
66
64
Binding Energy (eV)

References

[1] I. Dursun, M. De Bastiani, B. Turedi, B. Alamer, A. Shkurenko, J. Yin, A. M. El-Zohry, I. Gereige, A. AlSaggaf, O. F. Mohammed, M. Eddaoudi, O. M. Bakr, *ChemSusChem* **2017**, *10*, 3746.

[2] C. C. Stoumpos, C. D. Malliakas, J. A. Peters, Z. Liu, M. Sebastian, J. Im, T. C. Chasapis, A. C. Wibowo, D. Y. Chung, A. J. Freeman, B. W. Wessels, M. G. Kanatzidis, *Cryst. Growth Des.* **2013**, *13*, 2722.

[3] R. J. Elliott, *Phys. Rev.* **1957**, *108*, 1384.

[4] C. L. Davies, M. R. Filip, J. B. Patel, T. W. Crothers, C. Verdi, A. D. Wright, R. L. Milot, F. Giustino, M. B. Johnston, L. M. Herz, *Nat. Commun.* **2018**, *9*, 293.

[5] M. Saba, M. Cadelano, D. Marongiu, F. Chen, V. Sarritzu, N. Sestu, C. Figus, M. Aresti, R. Piras, A. Geddo Lehmann, C. Cannas, A. Musinu, F. Quochi, A. Mura, G. Bongiovanni, *Nat. Commun.* **2014**, *5*, 5049.